Carbon Dioxide Capture for Storage in Deep Geologic Formations – Results from the CO_2 Capture Project

Capture and Separation of Carbon Dioxide from Combustion Sources

Edited by

David C. Thomas
Senior Technical Advisor
Advanced Resources International, Inc.
4603 Clearwater Lane
Naperville, IL, USA

Volume 1

ELSEVIER
2005

Amsterdam – Boston – Heidelberg – London – New York – Oxford
Paris – San Diego – San Francisco – Singapore – Sydney – Tokyo

Elsevier Internet Homepage – http://www.elsevier.com
Consult the Elsevier homepage for full catalogue information on all books, major reference works, journals, electronic products and services.

Elsevier Titles of Related Interest

AN END TO GLOBAL WARMING
L.O. Williams
ISBN: 0-08-044045-2, 2002

FUNDAMENTALS AND TECHNOLOGY OF COMBUSTION
F. El-Mahallawy, S. El-Din Habik
ISBN: 0-08-044106-8, 2002

GREENHOUSE GAS CONTROL TECHNOLOGIES: 6TH INTERNATIONAL CONFERENCE
John Gale, Yoichi Kaya
ISBN: 0-08-044276-5, 2003

MITIGATING CLIMATE CHANGE: FLEXIBILITY MECHANISMS
T. Jackson
ISBN: 0-08-044092-4, 2001

Related Journals:
Elsevier publishes a wide-ranging portfolio of high quality research journals, encompassing the energy policy, environmental, and renewable energy fields. A sample journal issue is available online by visiting the Elsevier web site (details at the top of this page). Leading titles include:

Energy Policy
Renewable Energy
Energy Conversion and Management
Biomass & Bioenergy
Environmental Science & Policy
Global and Planetary Change
Atmospheric Environment
Chemosphere – Global Change Science
Fuel, Combustion & Flame
Fuel Processing Technology

All journals are available online via ScienceDirect: www.sciencedirect.com

To Contact the Publisher
Elsevier welcomes enquiries concerning publishing proposals: books, journal special issues, conference proceedings, etc. All formats and media can be considered. Should you have a publishing proposal you wish to discuss, please contact, without obligation, the publisher responsible for Elsevier's Energy program:

Henri van Dorssen
Publisher
Elsevier Ltd
The Boulevard, Langford Lane
Kidlington, Oxford
OX5 1GB, UK

Phone: +44 1865 84 3682
Fax: +44 1865 84 3931
E.mail: h.dorssen@elsevier.com

General enquiries, including placing orders, should be directed to Elsevier's Regional Sales Offices – please access the Elsevier homepage for full contact details (homepage details at the top of this page).

ELSEVIER B.V.
Radarweg 29
P.O. Box 211, 1000 AE Amsterdam
The Netherlands

ELSEVIER Inc.
525 B Street, Suite 1900
San Diego, CA 92101-4495
USA

ELSEVIER Ltd
The Boulevard, Langford Lane
Kidlington, Oxford OX5 1GB
UK

ELSEVIER Ltd
84 Theobalds Road
London WC1X 8RR
UK

First edition 2005

Library of Congress Cataloging in Publication Data
A catalog record is available from the Library of Congress.

British Library Cataloguing in Publication Data
A catalogue record is available from the British Library.

ISBN: 0-08-044570-5 (2 volume set)

Volume 1: Chapters 8, 9, 13, 14, 16, 17, 18, 24 and 32 were written with support of the U.S. Department of Energy under Contract No. DE-FC26-01NT41145. The Government reserves for itself and others acting on its behalf a royalty-free, non-exclusive, irrevocable, worldwide license for Governmental purposes to publish, distribute, translate, duplicate, exhibit and perform these copyrighted papers. EU co-funded work appears in chapters 19, 20, 21, 22, 23, 33, 34, 35, 36 and 37. Norwegian Research Council (Klimatek) co-funded work appears in chapters 1, 5, 7, 10, 12, 15 and 32.

Volume 2: The Storage Preface, Storage Integrity Preface, Monitoring and Verification Preface, Risk Assessment Preface and Chapters 1, 4, 6, 8, 13, 17, 18, 19, 20, 21, 22, 23, 24, 25, 26, 27, 28, 29, 30, 31, 32, 33 were written with support of the U.S. Department of Energy under Contract No. DE-FC26-01NT41145. The Government reserves for itself and others acting on its behalf a royalty-free, non-exclusive, irrevocable, worldwide license for Governmental purposes to publish, distribute, translate, duplicate, exhibit and perform these copyrighted papers. Norwegian Research Council (Klimatek) co-funded work appears in chapters 9, 15 and 16.

♾ The paper used in this publication meets the requirements of ANSI/NISO Z39.48-1992 (Permanence of Paper).
Printed in The Netherlands.

Carbon Dioxide Capture for Storage in Deep Geologic Formations, Volume 1
D.C. Thomas and S.M. Benson (Eds.)

Chapter 19

GRACE: DEVELOPMENT OF Pd–ZEOLITE COMPOSITE MEMBRANES FOR HYDROGEN PRODUCTION BY MEMBRANE REACTOR

M. Menéndez[1], M.P. Pina[1], M.A. Urbiztondo[1], L. Casado[1], M. Boutonnet[2], S. Rojas[2] and S. Nassos[2]

[1]Department of Chemical and Environmental Engineering, Faculty of Sciences, University of Zaragoza, 50009 Zaragoza, Spain
[2]Department of Chemical Engineering and Technology, The Royal Institute of Technology (KTH), Teknikringen 42, 100 44 Stockholm, Sweden

ABSTRACT

Pd–zeolite composite membranes have been prepared over the external surface of macroporous α-alumna tubular supports by secondary growth of zeolite layers followed by Pd modification. Pd nanoparticles (few nanometers in size) filtration and/or impregnation + in situ reduction of an organic Pd precursor have been explored as deposition techniques devoted to enhance the H_2 separation performance of the non-defect free A-type zeolite membranes. The Pd deposition aims toward the partial blockage of the non-selective inter-crystalline pathways, which may account for a significant fraction of the total permeation flux. The Pd–zeolite composite substrates have been characterized by XRD, SEM and EDX. The study of the permeation properties of these substrates for single (N_2) and binary mixtures (H_2–CO_2) before and after Pd modification, reveals some improvements in terms of H_2 separation performance. The impregnation + in situ reduction of palladium acetylacetonate solution ($Pd(acac)_2$) carried out over KA zeolite membranes previously seeded with Pd nanoparticles appears as the most adequate among the tested methods. Separation factors for H_2-CO_2 binary mixtures up to 145 have been achieved, although further optimization is required to improve the H_2 permeation fluxes (around 10^{-8} mol H_2/m^2 s Pa).

INTRODUCTION

Zeolite supported membranes have been extensively developed over the last two decades due to their potential applications as membrane separators, membrane reactors and selective sensors due to the intrinsic properties of zeolites and the advantages of a membrane-type configuration [1–8]. Zeolites are microporous crystalline materials with a uniform pore size distribution at molecu4lar scale. This affords strong molecule–membrane interaction and makes them excellent candidates for separation applications based on molecular sizes. Ideally, zeolite membranes can sieve out molecules at high temperature, although permeation of molecules larger than the zeolitic pore size is sometimes observed due to the presence of non-selective inter-crystalline defects. Therefore, a continuous defect-free zeolite layer is required for the optimal operation of the membrane separation system, i.e. control of this non-zeolitic pathway is needed. However, differences in chemical nature, molecule size and shape, and adsorption/diffusion in the zeolite channels can also account for high separation selectivities between components of various mixtures such as hydrocarbon isomers, water/organics, etc.

The MFI membrane is the most often zeolite type prepared as a membrane due to the accumulated knowledge in the synthesis of MFI structure, the relative ease preparation and the relative high thermal and chemical stability (high SiO_2/Al_2O_3 ratio). For permanent gases or permanent/hydrocarbon mixtures separation, MFI type zeolite membranes have not shown good performance because of the large pore size and their hydrophobic nature. In addition to MFI membranes, different types of zeolite membranes,

e.g. A, FAU, MOR, FER have been synthesized over the last two decades [9–15]. In particular, A-type zeolite membranes (channel opening size of 0.41 nm for NaA zeolite and 0.35 nm for K zeolite) offer promising separation possibilities.

Various processes for production and purification of hydrogen have attracted much attention world-wide [16] because hydrogen is emerging as an important energy resource to meet environmental requirements and also as primary feedstock for the petrochemical industry. Dense membranes, either as Pd or Pd alloys, have so far provided the best selectivity for hydrogen separation [17–26]; however, the low permeation fluxes of a Pd membrane with enough mechanical stability and the high price of Pd make the search for alternative materials economically attractive.

In this context, A-type zeolite membranes could in principle be a competitive alternative to separate H_2 from hydrocarbons, in view of the larger kinetic diameter of these (e.g. about 0.43 nm for *n*-paraffins); but some difficulties arise because the presence of inter-crystalline voids may account for a significant fraction of the total permeation flux. The probability of defects increase with membrane dimensions and the synthesis of sufficiently large membranes structures with a low concentration of defects remains the main obstacle for industrial applications. Although it has been shown that a good selectivity can sometimes be obtained with imperfect zeolite membranes [27], gas phase separations in the size exclusion (molecular sieving) regime require membranes of an exceptionally good quality. Furthermore, the difficulty in achieving a thin and almost defect-free zeolite film increases for systems with a large Al/Si ratio as in the case of A-type zeolite where this value is around one.

Some reparation methods have been described in the literature in order to diminish the inter-crystalline defect size. One option is to fill the non-selective pathway with amorphous silica or other materials by chemical vapor deposition [28] or by coke deposition [29]. Other possibilities rely on new synthesis methods for successful membrane formation. Proper conditions are necessary to allow for preferential nucleation and growth of zeolite crystals on the support surface (possibly competing with solution events). The technique referred to as secondary (seeded) growth, involves attaching a closely packed layer of zeolite seed crystals on the surface of a support which act as nuclei for further crystal growth under suitable hydrothermal conditions to fill the inter-crystalline space [30–32]. However, during secondary growth, the reactant mixture in contact which the tubular porous support, changes in composition with time provoking a reduction of the membrane quality, reproducibility and problematical scale-up. Some authors propose as alternatives the continuous synthesis of zeolite membranes [33–35] or the direct heating of the substrate while the reaction mixture is kept at lower temperature [36,37]. In this manner, the reaction is suppressed in the bulk and promoted on the surface, and the phase transformations of metastable materials can be delayed. Some authors have attempted to use centrifugal forces to drive the crystal nuclei formed in the homogeneous phase toward the support [38], promoting the formation of a more continuous and dense zeolite layer.

Nevertheless, the relative few gas permeation studies reported for NaA zeolite [39–45], in comparison with publications focused on pervaporation [38,42,46–51], show a poor quality zeolite membrane even when synthesized on disk supports.

In a previous work [52] we proposed a novel approach to solve this problem, which consisted on the blocking of the non-selective inter-crystalline pathways by a selective material (Pd). In this work, microporous layers of zeolite K synthesized over the external surface of tubular substrates have been modified with Pd deposited by different techniques: vacuum impregnation of Pd nanoparticles, cross-flow filtration of Pd nanoparticles from microemulsions, impregnation + "in situ" reduction of a commercial metal–organic precursor and their possible combinations. Although the preparation of Pd nanoparticles and the synthesis of zeolite layers are different techniques, we have considered that in this chapter both techniques will be presented jointly, since the aim is to develop procedures for including the nanoparticles in the membrane structure. These procedures could block inter-crystalline defects by Pd, while maintaining free zeolite channels. In such a way, a structure in which the selective zeolite pores are preserved and non-selective voids are blocked by Pd would certainly be attractive for H_2 permeation compared to existing Pd metallic membranes: considerable Pd savings could be obtained and the resulting membrane would be more robust against thermal cycling. With this approach, high fluxes of hydrogen

could be obtained, while maintaining the selectivity of the membrane. This approximation presents an enormous potential not only for separation applications in view of the growing interest of H_2 as a clean fuel but also for coupled reaction and separation processes as water–gas shift, steam reforming of hydrocarbons or dehydrogenations.

EXPERIMENTAL / STUDY METHODOLOGY

Microporous A-Type Zeolite Membrane Preparation and Characterization

Preparation of A-type zeolite membranes

Zeolite NaA membranes were hydrothermally synthesized on the external surface of α-alumna symmetric tubes of 7 mm ID and 10 mm OD, with a nominal pore size of ~1900 nm. These supports, previously subjected to enameling at both ends defining a permeation length of approximately 5 cm, were externally seeded by rubbing with pure zeolite A crystals with a mean size of 1 μm. Secondary growth of the seed layer deposited on the support tubes was carried out for 5 h at approximately 90 °C using a nutrient solution with a molar composition of $80Na_2O\text{-}1Al_2O_3\text{-}9SiO_2\text{-}5000H_2O$ according to the recipe of Kumakiri et al. [13].

Figure 1 shows the experimental set-up used in this work for zeolite membrane synthesis, consisting basically on an open teflon flask with four individual sections, which allow us to carry out synthesis at 90 °C during 5 h over four different supports at once. In any case, several cycles are necessary to reach suitable permeation levels with low contribution of laminar flow. After each synthesis, the tubes were rinsed in distilled water and dried from room temperature up to 150 °C in an electrical oven, following a heating procedure described under "Results and Discussion", to avoid the uncontrolled loss of water from this highly hydrophilic zeolite.

In order to reduce the aperture of the selective zeolitic channels (from 0.41 to 0.35 nm), NaA zeolite membranes have been exchanged to their K counterparts [53]. The experimental procedure for sodium–potassium exchange has been established from a previous experience which is fully described in "Results and Discussion".

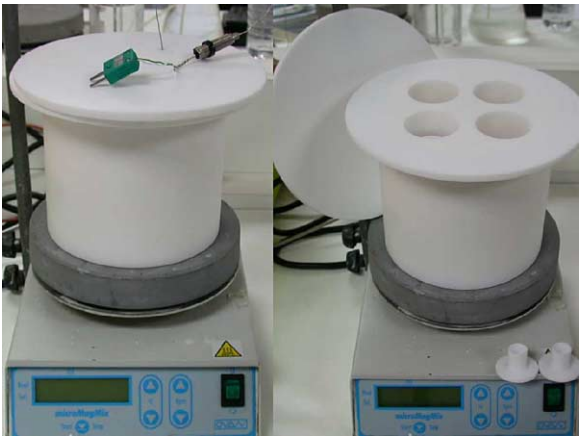

Figure 1: Experimental set-up for the synthesis of A-type zeolite membranes.

Characterization of A-type zeolite membranes

The phases present in the A-type zeolite membranes were characterized by X-ray diffraction (XRD) analysis (Rigaku/Max diffractometer CuKα radiation and graphite monochromator) of the membrane top layers. Morphology characterization of the as prepared membranes were also examined by scanning electron microscopy (SEM) (JEOL JSM-6400 operating at 20 kV).

The permeation properties of the prepared membranes, i.e. single gas permeance, laminar contribution to total permeation flux, separation factor and size distribution of effective pores for diffusion; have been measured by means of three different equipments.

- The contribution of the laminar and Knudsen permeation to the total flux was measured by following the transient pressure in the retentate side after the communication between this side of the membrane and a closed vessel was suddenly opened (Figure 2A).
- The permeation of gases at several temperatures (H_2, CO_2 and their binary mixtures) was evaluated by analyzing on-line the retentate and permeate with a mass spectrometer or a gas chromatograph. Ar was used as sweep gas, and a feed/sweep gas ratio around one was always employed keeping the same total pressure at both sides of the membrane (Figure 2B).
- The contribution of pores with different size to the gas permeation was evaluated by permporometry analysis using water as condensable vapor. In this technique the N_2 permeation was measured at different values of relative humidity for the permeating stream (Figure 2C). By assuming that water was condensed in the pores with a size given by the Kelvin equation, the permeation through pores larger than this value was accounted. In this way, the pore size distribution, for those pores that effectively contribute to the gas permeation, was obtained.

Pd–Zeolite Composite Membranes

Seeding with Pd nanoparticles

Pd nanoparticles from microemulsions or organic solutions have been filtered over A-type zeolite membranes in order to activate the surface with palladium nuclei. In such way, palladium particles, acting as

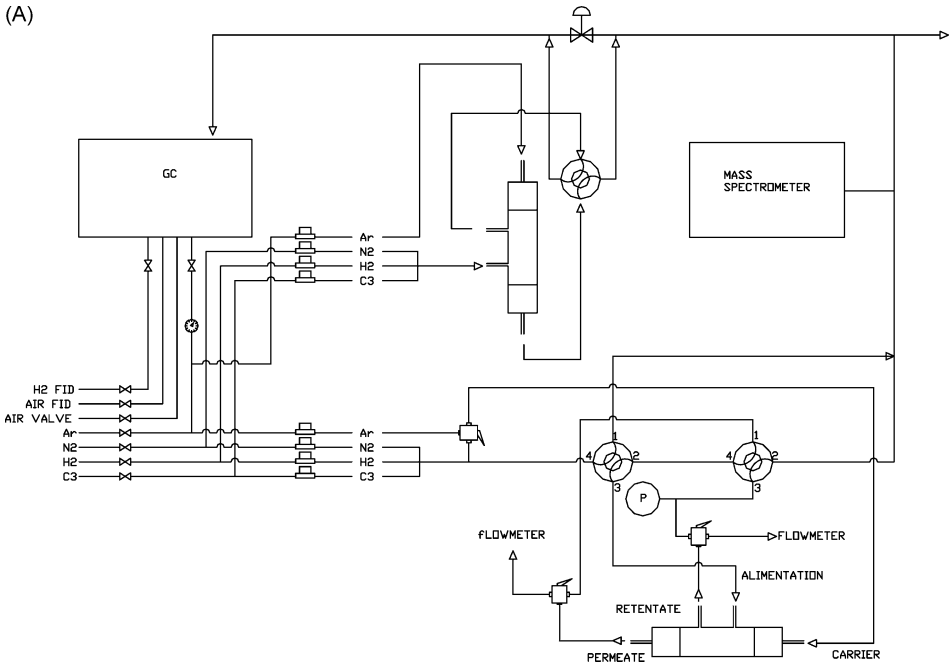

Figure 2: Experimental set-up for A-type zeolite membranes characterization by: (A) permeation properties evaluation for single and binary mixtures, (B) Knudsen and laminar contributions to total permeation flux, (C) permporometry analysis.

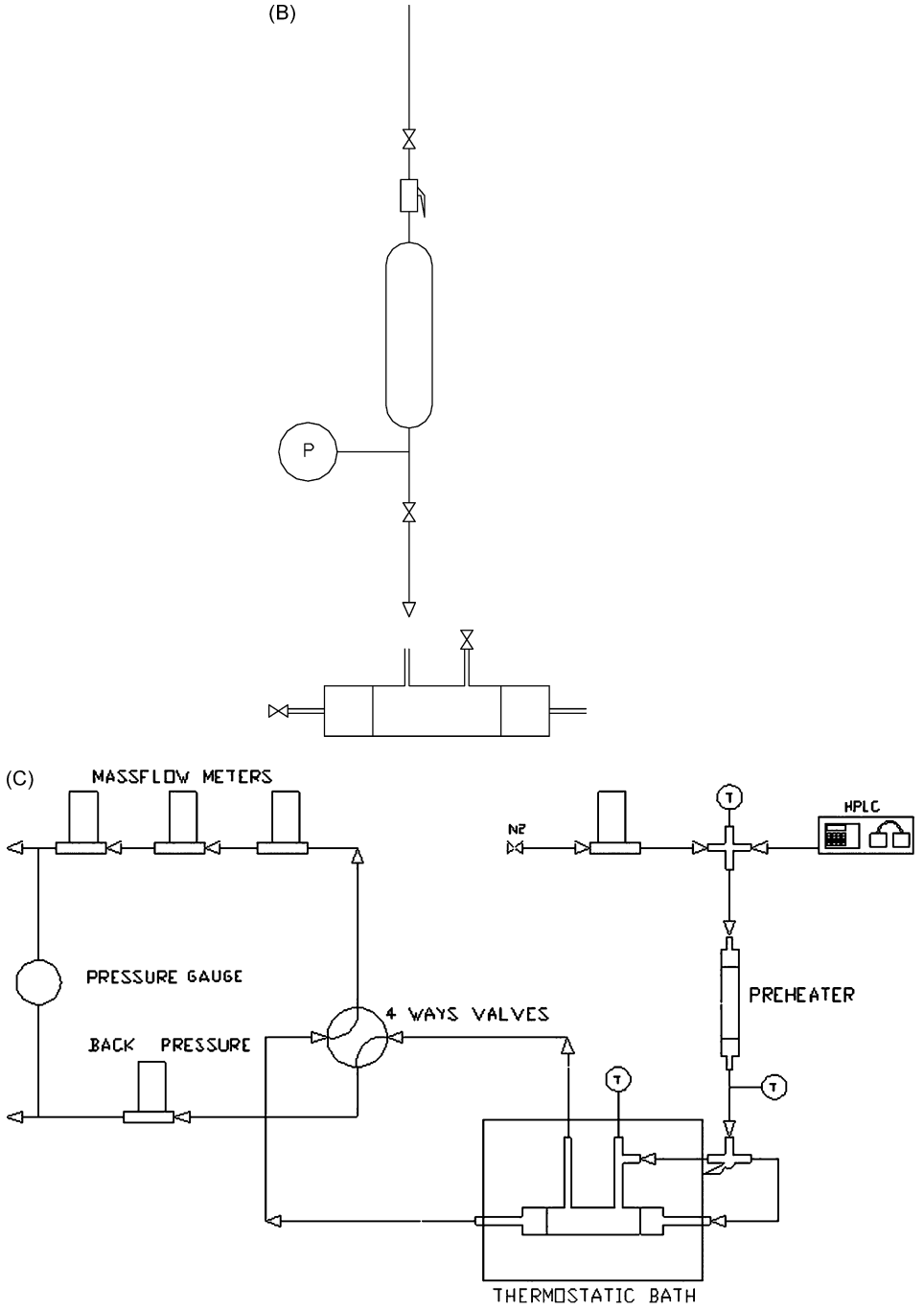

Figure 2: Continued.

seeds for further growth, are dispersed in the mesopores located in the non-defect free zeolite layer, facilitating a more homogenous deposition during the subsequent stages of Pd modification.

Palladium Seeding by Microemulsion Filtration

Preparation of Pd nanoparticles

One of the techniques employed for Pd nanoparticles preparation with suitable physical and chemical properties in order to being deposited onto defective zeolite membrane layers for conferring selectivity towards specific gas molecules was based on our previous experience in microemulsions [54–56]; due to the fact that metal particles with size ranging from 2 to 9 nm are easily obtained.

The preparation method usually involves the addition of a Pd salt, previously dissolved in water, to an oil/surfactant mixture under vigorous stirring. Reduction of the Pd particles is performed in situ by hydrazine addition.

The influence of metal source has been studied by using two different sets of Pd precursors: $PdCl_2$ (99.9 + %, Aldrich) which is only soluble at acidic pH values, and $Pd(NH_3)_4Cl_2{\cdot}H_2O$ (99.9%, Alfa Aesar). Additionally, the effect of the oil phases and surfactants has also been investigated: (i) non-ionic surfactants: Berol 050 (Alcoholethoxylate, Akzo Nobel), Berol 020 (Nonylphenol ethoxylate, Akzo Nobel) and Tween® 65 (Polyoxyethylenesorbitan Tristearate, Sigma-Aldrich); (ii) ionic surfactants: CTAB (Cetyl Trimethyl Ammonium Bromide, Aldrich) in combination with 1-butanol as co-surfactant (99.9%, Aldrich); and (iii) oil phases: isooctane (2,2,4-Trimethylpentane, HPLC 99.7 + %, Alfa Aesar) and cyclohexane (99.5 + %, Aldrich).

Therefore, a wide variety of microemulsion systems has been prepared and analyzed by TEM in terms of Pd particle size and shape distribution (results out of the scope of this work). Table 1 summarizes the conditions used for the Pd microemulsion preparation here employed which render in particle sizes from 5 to 9 nm as is confirmed by TEM analysis (not shown here). The as prepared Pd–zeolite composite membranes (Table 2) were identified by MNaMI or MKMI prefix depending on the ionic zeolite form.

TABLE 1
CHARACTERISTICS OF THE MICROEMULSION USED FOR Pd NANOPARTICLES PREPARATION

Phase	Constituent	wt%
Metal precursor	$Pd(NH_3)_4Cl_2$ H_2O	0.1% Pd
Reducing agent	Hydrazine	4.9% H_2O
Oil	Isooctane	74.9% Oil
Surfactant	Berol 050	20% Surfactant

Deposition of Pd nanoparticles

The deposition into the microporous zeolite membranes has been achieved by using the zeolite membranes as a filter of Pd nanoparticles either from a microemulsion or from a de-stabilized/re-dispersed suspension in ethanol. The latter Pd source has been tested in order to overcome the problems that might arise from the presence of an organic surfactant able to decompose with temperature altering the permeation properties of the composite membranes. Therefore, some substrates have been prepared using Pd nanoparticles recovered after microemulsion de-stabilization (by using ethanol) and re-dispersed again in ethanol using an ultrasonic bath.

The filtration has been carried out at room temperature using three different experimental set-ups (method 1, 2 and 3, respectively) in order to analyze the effect of transmembrane pressure, Pd source, filtration

TABLE 2
MAIN CHARACTERISTICS OF THE ZEOLITE MEMBRANES PREPARED FOR THIS WORK

Sample	No. cycles	Weight gain (mg /g)	Before K exchange		After K exchange	
			mol N_2/m^2 s Pa	% Lam. Contr.	mol N_2/m^2 s Pa	% Lam. Contr.
MNaMI1	3	12.7	6.7×10^{-8}	35	–	–
MNaMI2	3	10.2	1.3×10^{-7}	10	–	–
MNaMI3	2	11.4	4.7×10^{-9}	33	–	–
MNaMI4	2	11.3	1.7×10^{-8}	22	–	–
MNaMI5	2	12.3	6.5×10^{-8}	20	–	–
MKMI1	4	5.4	1.1×10^{-8}	20	3.2×10^{-7}	20
MKMI2	4	7.4	6.9×10^{-8}	21	7.2×10^{-7}	23
MKMI3	4	7.7	4.9×10^{-7}	33	8.7×10^{-7}	18
MKMI4	1	12.4	1.1×10^{-7}	13	9.9×10^{-8}	10
MKMI5	1	9.4	2.4×10^{-7}	27	4.4×10^{-8}	26
MKN1	2	10.9	2.4×10^{-8}	14	2.1×10^{-6}	9
MKN2	1	6.8	5.7×10^{-8}	20	5.8×10^{-7}	7
MKN3	1	6.5	3.8×10^{-8}	17	7.0×10^{-8}	20
MKN4	2	7.9	2.0×10^{-8}	11	6.4×10^{-7}	21
MKN5	4	6.9	2.0×10^{-8}	9.5	5.1×10^{-7}	14
MKN6	4	–	4.0×10^{-8}	14	6.5×10^{-7}	10
MKN7	3	3.0	7.6×10^{-8}	17	3.9×10^{-7}	14
MKN8	5	8.6	1.9×10^{-8}	30	4.2×10^{-7}	24
MKN9	1	7.1	1.4×10^{-8}	25	8.2×10^{-8}	–
MKN10	1	5.7	9.5×10^{-8}	25	7.4×10^{-8}	13

duration (from 4 to 72 h) over the membrane permeation properties modification. Some preliminary conclusions are summarized under "Results and Discussion". After Pd deposition, all the membranes were thoroughly washed with ethanol and dried at 110 °C overnight.

Method 1: non-continuous vacuum filtration in a stainless-steel module "NCVF". According to this method, the zeolite membrane is mounted into a stainless steel module, similar to the one shown in Figure 2A. After an adequate vacuum is reached downstream (2×10^{-3}mbar), the communication between the feed side of the membrane and the closed vessel containing the Pd source is suddenly opened. For this configuration, a de-stabilized/re-dispersed suspension in ethanol has been used as Pd source. The filtration is prolongued for a couple of hours, and several cycles are necessary to ensure that a significant amount of Pd particles has been homogenously incorporated onto the membrane surface.

Method 2: continuous vacuum filtration in a glass reactor "CVF". For this approach, the zeolite membrane is placed inside a glass chamber filled with the Pd microemulsion. In a similar way to method 1, the internal side of the membrane is connected by suitable swagelok fittings to the vacuum pump whereas the external side (where the zeolite layer is located) is kept in contact with the Pd source. This configuration has also been used for Pd seeding by nanoparticles organic solution filtration.

Method 3: high pressure/vacuum filtration in a stainless-steel module "HPF". This method is rather similar to method 1 with the exception that the microemulsion, connected to the feed side of the membrane by means of an on–off valve, is placed in a pressurized vessel (up to 5 barg).

Pd microemulsion characterization by thermogravimetry

The main objective of the Pd microemulsions thermo-gravimetric analysis (TGA) was to determine the calcination conditions required for the successful elimination of the surfactant (Berol 050) and water/oil phase from the surface of the membranes. Complete removal of these organic compounds will prevent the formation of cracks and pinholes on the membrane surfaces, which will eventually result in a better H_2 separation performance.

The studied experimental variables have been the oxygen concentration in the gas stream (2 and 20% with N_2 as balance) and the final calcination temperature (from 250 to 350 °C). A common protocol was established for all the analyses, which consists of: (i) heating up to 100 °C at 0.5 °C/min under 2% O_2, (ii) a first dwell at 100 °C for 2 h, (iii) heating up to 150 °C at 0.5 °C/min under 2% O_2, (iv) a second dwell at 150 °C for 2 h, (v) heating up to 200 °C at 0.5 °C/min under 2% O_2, and (vi) a third dwell at 200 °C for 2 h. After these stages, the stream composition could be shifted from 2% O_2 (Protocol 1) to 20% O_2 (Protocol 2). Protocol 3, involving air atmosphere throughout all the above mentioned heating steps, was also tested. For the three protocols, the final calcination temperature was further increased up to 350 °C until no weight change was detected.

Palladium Seeding by Nanoparticles Organic Solution Filtration

Preparation of Pd nanoparticles

A redox-controlled method [57] has also been employed for the size selective preparation of Pd-colloids in which tetraoctylammonium bromide and palladium acetate are used as reactants in tetrahydrofurane (THF) media at 66 °C. Acetate induces rapid metal reduction, which favors the formation of a black metal colloid solution of stabilized Pd-clusters rather homogenous in size (3.3 ± 0.6 nm [58]). The as prepared Pd–zeolite composite membranes were identified by "MKN" prefix (Table 2).

Deposition of Pd nanoparticles

Since the stabilized Pd nanoparticles cannot enter the zeolite pore network, it is expected that Pd would be entrained in the filtration flow, leading to a preferential deposition in the inter-crystalline voids. A 0.3 mM solution of Pd nanoparticles in tetrahydrofurane was filtered through the A-type zeolite membranes using the above described method 2. Several filtration cycles (12 h each) were carried out; in each of them, the suspension of Pd nanoparticles contacted the membrane outer (zeolite layer) side, while maintaining the inner (permeate) side at a moderate vacuum (10^{-2} mbar). Liquid nitrogen traps were placed downstream to condense the vapors permeated across the membrane, but no metal particles were detected in the liquid collected.

Pd deposition by impregnation + in situ reduction "IRIS technique"

A novel method for Pd deposition over porous membranes has been developed and presented for the first time in this work. The concept is based on the employment of the zeolite membrane as interfacial contactor [59,60] between the gas phase carrying the reducing agent (H_2) and the liquid phase (dichloromethane) in which the Pd precursor ($Pd(acac)_2$) is dissolved. Both reactants are fed from opposite sides of the tubular support to the defective zeolite layer. The experimental set up is shown in Figure 3A. The configuration plotted in Figure 3B is suitable for zeolite membranes synthesized on the external side of the support. In such a way, the liquid phase penetrates inside the porous structure by capillary forces up to the zeolite layer, whereas the gas phase is continuously sweeping the external surface, promoting the solvent evaporation and simultaneously the Pd reduction. The location of the reaction interface depends on the experimental conditions, which must be tuned to shift the reduction interface where the non-selective defects are predominant. It is worth to emphasize that this technique does not demand high temperatures, allows us to carry out the impregnation and in situ Pd reduction at once and its versatility lets the modification of the Pd pattern deposition varying the solvent, reaction temperature, gas flow-rate, hydrogen partial pressure, transmembrane pressure or Pd concentration in the liquid phase.

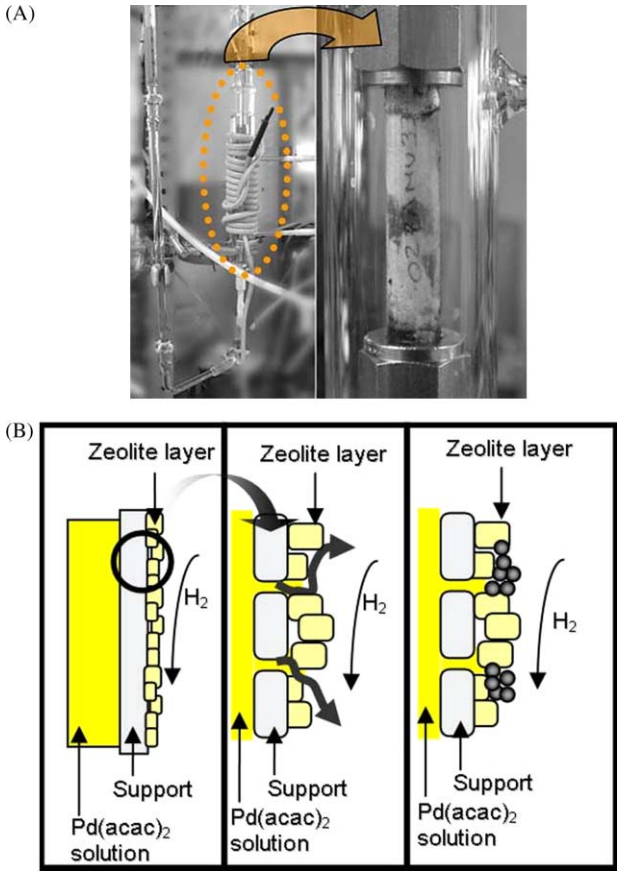

Figure 3: Experimental set-up for Pd deposition by impregnation + in situ reduction "IRIS" technique: (A) IRIS system, (B) process scheme.

RESULTS AND DISCUSSION

Microporous A-Type Zeolite Membrane Preparation and Characterization

Table 2 compiles the synthesis conditions, zeolite loadings, single N_2 permeances and percentages of laminar contribution to total permeation fluxes (evaluated according to the equation proposed by Keizer et al [61]) of the membranes prepared for this work. All of them have been seeded by rubbing with commercial zeolite A crystals (1 μm as average size). SEM micrographs shown in Figure 4, correspond to the topside and cross section view of a seeded support. As it can be observed, the coverage degree is rather homogeneous; and the seed size employed favors the penetration of the zeolite crystals among the alumna grains of the starting substrate, facilitating the posterior adhesion of the zeolite layer.

For identification purposes, the NaA zeolite membranes samples were denoted using "MNa" prefix, whereas "MK" was used for the potassium-exchanged form. The permeation properties tabulated have been measured after a controlled drying at 150 °C overnight.

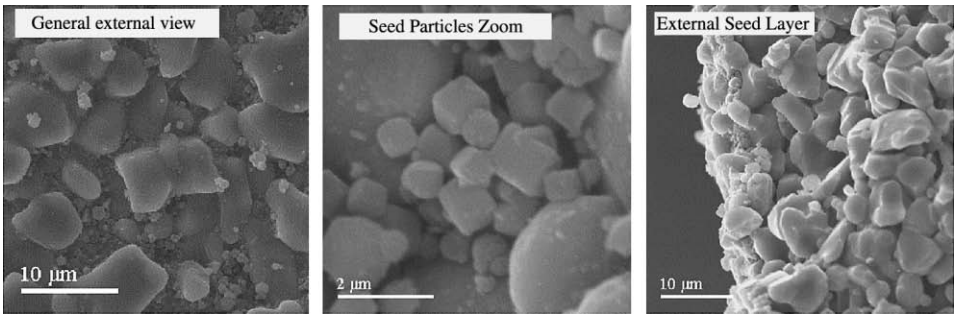

Figure 4: SEM micrographs of commercial tubular supports (1900 nm as nominal pore size) after seeding with commercial A zeolite crystals (1 μm size) by rubbing.

The experimental procedure for sodium–potassium exchange has been established from a previous experience in which the influence of exchange period over the percentage of Na exchanged was studied. For such experiment, a standard NaA zeolite membrane was divided into four pieces, each of them was further subjected to different contact times with the KCl solution. Table 3 summarizes the ICP results corresponding to the Si, Na and K analyses of the corresponding solutions after the ionic exchange with 0.1 M KCl as starting exchange solution using a ratio of solution volume (cm^3)/porous membrane length (cm) equal to 20. Under such conditions, 24 h of contact time ensures a 92% of Na exchanged; therefore, this value has been kept for all the KA membranes prepared for this work.

The drying protocol was adopted due to the fact that thermal cracks were produced when conventional heating were used, as is evidenced by the SEM analysis shown in Figure 5A–C. Figure 5A corresponds to the external surface of a standard NaA zeolite membrane subjected to a controlled drying procedure. The zeolite crystal aggregates, globular in shape, result from the successive synthesis cycles carried out in order to adequate the permeation properties. Figure 5B and C correspond to an uncontrolled dried sample for which typical thermal expansion cracks (up to 0.4 μm in thickness) are observed.

The membrane thermal stability study carried out (Figure 6), reveals that the maximum temperature that this type of material can withstand is 350 °C. At this temperature, the percentage of laminar contribution remains constant whereas N_2 permeance increases 50% with respect to 150 °C, probably as a consequence of chemisorbed water removal. Moreover, SEM analysis (not shown here) reveals that the inherent thermal cracks formation, due to the opposite expansion coefficients of the support and the zeolite layer respectively, is avoided; preserving the zeolite membrane integrity.

Therefore, although significant amounts of water could remain adsorbed in the micropores for the permeance measurements tabulated, the laminar contributions given in Table 2 can be used as a general-purpose quality control method. A significant concentration of defects translates into larger laminar contributions, even at low N_2 permeances, probably caused by the presence of amorphous silica over the external surface of the zeolite layer. As it can be observed, when different samples are compared, even those subjected to the same number of synthesis cycles, a limited reproducibility in single gas permeation properties for A-type zeolite membranes is detected (from 4.7×10^{-9} to 2.4×10^{-7} mol N_2/Pa s m^2 and 9.5–35% of laminar contribution to total N_2 permeation flux); although the weight gains vary in a relative narrow range (from 3.0 to 12.7 mg/g expressed per total membrane weight). For average values of 9.2×10^{-8} mol N_2/Pa s m^2 and 21.2% of laminar contribution, permporometry measurements using water as condensable vapor, indicate that around 52% of the total N_2 permeation flux is through micropores, i.e. pores smaller than 2 nm, and 80% through pores smaller than 10 nm.

Figure 7 shows the diffractograms obtained from the XRD analysis of the external surface of standard NaA and KA zeolite membranes. The comparison with pure NaA zeolite pattern [62] shows that zeolite with

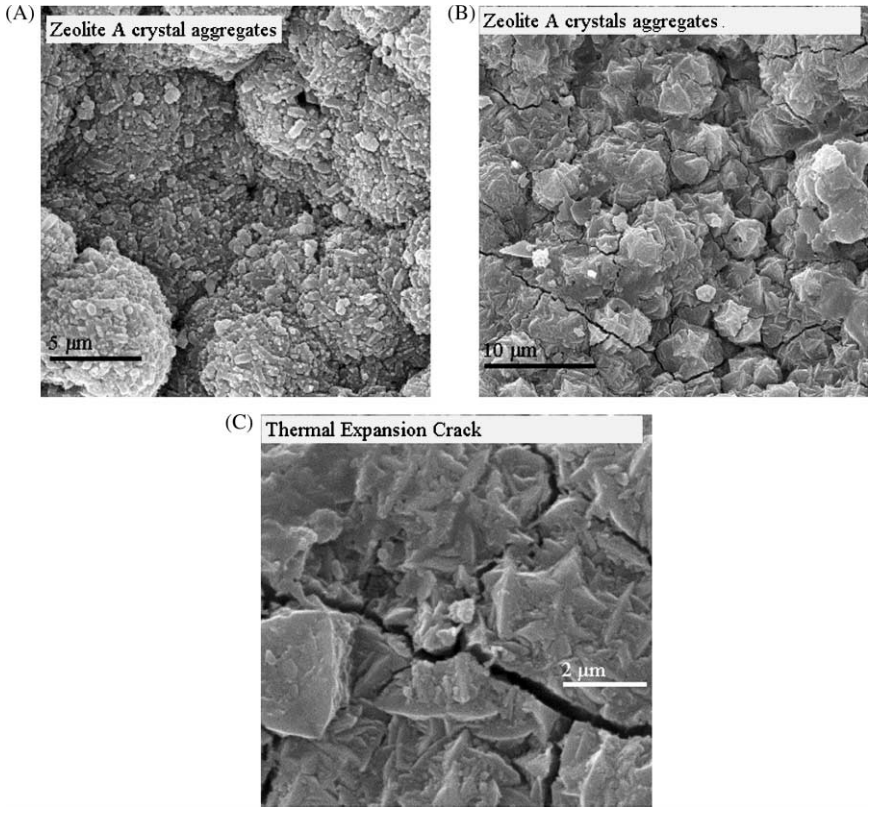

Figure 5: SEM micrographs of external surface of type A zeolite membranes subjected to different drying procedures at final temperatures of 150 °C: (A) controlled drying procedure, (B) uncontrolled drying procedure, (C) magnification of a thermal expansion crack.

the LTA-type structure is present in the KA sample; whereas for the sodic form, the only quantitative diffraction detected, in the measured range, is associated with the α-alumna support (at 25.9°). Moreover, when both membrane top layers were analyzed by SEM (Figure 8), it is observed that K-exchanged membrane seems better crystallized than the preceding NaA form. These observations correlate quite well with the evolution of permeation properties with the K-exchange shown in Table 2. With the exception of MKMI4, MKMI5 and MKMI10 samples, the N_2 permeances of all the membranes increases up to two orders of magnitude after K exchange (e.g. MKN1). A possible explanation could rely on the partial leaching of non-well crystallized material during the potassium exchange, mainly amorphous silica according to the ICP analysis compiled in Table 3 (i.e. the exchange solutions revealed the presence of Si, about 0.07 g of Si per gram of Na exchanged). Nevertheless, an improvement in terms of non-selective pathways is observed after K-exchange according to the laminar contributions measured.

Pd–Zeolite Composite Membranes

Seeding with Pd nanoparticles

Table 4 summarizes the permeation properties after Pd deposition from microemulsion (MKMI and MNaMI samples) or Pd-THF solution (MKN samples) filtrations, respectively. The effect of filtration method (NCVF, CVF and HPF) is fully discussed in "Palladium Seeding by Microemulsion Filtration". However, for almost all the samples compiled, a notable reduction in single N_2 permeances after Pd

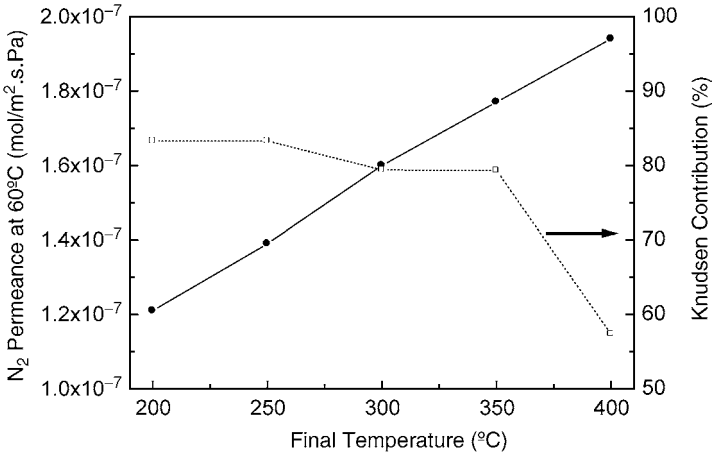

Figure 6: Evolution with temperature of N_2 permeance and Knudsen contribution for a standard A-type zeolite membrane.

filtration is evaluated, more noticeable when Pd nanoparticles from microemulsion are deposited (i.e. complete blocking of the membrane to gas permeation for MNaMI3 and MNaMI4, respectively). This effect agrees with a progressive reduction of the inter-crystalline defects and non-selective pathways for gas diffusion by Pd clusters and/or surfactant agent.

In order to overcome the problems that might arise from the presence of an organic surfactant (Berol) in the microemulsion, susceptible of decomposition at elevated temperatures, a suitable procedure for Berol removal which preserves the zeolite membrane quality has been investigated in this work. For that purpose, TGA analysis of Pd microemulsions, permeation studies with temperature of Pd–zeolite composite membranes prepared by microemulsion filtration and SEM analysis have been carried out in order to establish the minimum temperature necessary for the organic removal.

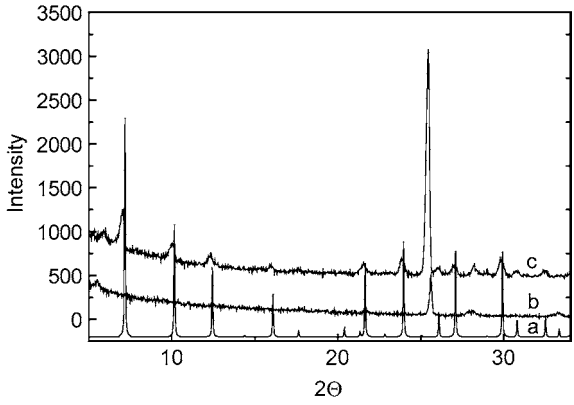

Figure 7: XRD spectra of A-type zeolite membrane top layers: (a) pure NaA zeolite pattern, (b) NaA zeolite membrane, (c) KA zeolite membrane.

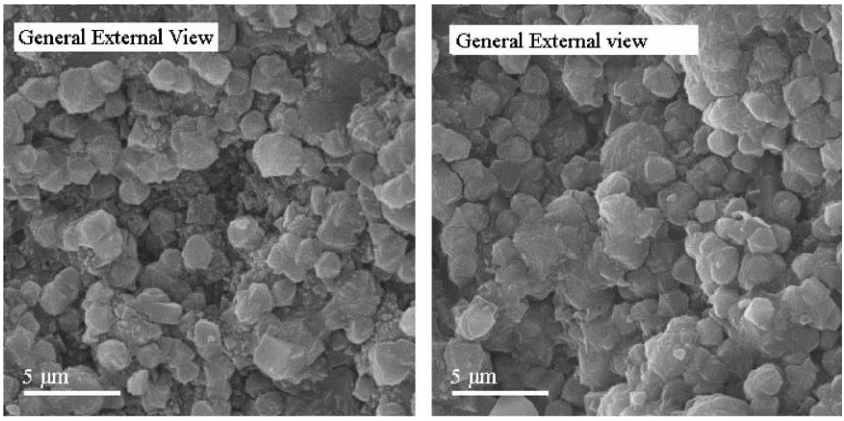

Figure 8: SEM micrographs of type A zeolite membranes: left side) before K exchange, right side) after K exchange.

TABLE 3
ICP ANALYSIS OF THE KCl SOLUTIONS AFTER THE Na-K IONIC EXCHANGE OVER A STANDARD NaA ZEOLITE MEMBRANE

Exchange period (h)	Si (mg/l)	Na (mg/l)	K (mg/l)	% Na exchanged
0		5.75	3967	0
12	3.54	100	3984	71.5
24	8.18	128	3828	92.3
36	5.93	138	3938	100

Figure 9 shows the evolution of transmembrane pressure, monitored on line using the experimental set up shown in Figure 2A, with temperature for a given air flow rate using a flow-through configuration for a Pd seeded zeolite membrane by microemulsion filtration subjected to a heating rate of 0.5 °C/min. The results obtained indicate that surfactant elimination starts at 250 °C when the pressure drop decreases in a 50% as a consequence of the organic elimination from the porous network.

Moreover, it is observed that Berol removal leads to Pd aggregates with a "sponge like" porous structure (Figure 10) suitable for further Pd growth, although cracks formation is unavoidable when the calcination continues up to 400 °C. Consequently, 250 °C has been used for Berol removal from all the MNaMI and MKMI membranes prepared for this work. Under such conditions, a slight improve in H_2 separation performance for Pd–zeolite composite membranes after Berol removal is observed (see Table 4), reaching H_2/CO_2 separation factors up to 10.5 (for MKMI1 sample) maintaining relative high H_2 permeances (5.5×10^{-7} mol H_2/Pa s m^2). However, although a significantive improvement has been attained, further reparation treatments are still necessary for total blockage of non-selective pathways.

Palladium Seeding by Microemulsion Filtration

From the comparison of the different filtration methods used with Pd microemulsions, some qualitative conclusions could be extracted. A preferential Pd deposition over the membrane surface closed to the stainless steel module inlets takes place when NCVF with a de-stabilized/re-dispersed Pd in ethanol is employed. CVF is the most favorable to get homogenous membranes with a unique filtration cycle for

TABLE 4
Pd–ZEOLITE COMPOSITE MEMBRANES PREPARED BY Pd NANOPARTICLES DEPOSITION

Sample	Filtration method	After filtration mol N_2/m^2 s Pa	After Berol removal[a]	
			mol H_2/m^2 s Pa	H_2/CO_2 selectivity
MNaMI1	HPF(72)	2.8×10^{-9}	7.6×10^{-8}	7.5
MNaMI2	HPF(24)	6.2×10^{-9}	3.8×10^{-7}	7
MNaMI3	CVF(24)	Gas-tight	8.9×10^{-8}	8
MNaMI4	HPF(8)	Gas-tight	7.3×10^{-8}	7
MNaMI5	CVF(8)	9.5×10^{-10}	1.3×10^{-7}	5.5
MKMI1	CVF2(4)	2.6×10^{-9}	5.5×10^{-7}	10.5
MKMI2	NCVF	1.7×10^{-8}	1.3×10^{-6}	4
MKMI3	CVF(8)	2.2×10^{-7}	8.1×10^{-7}	5
MKMI4	HPF(8)	2.6×10^{-7}	8.1×10^{-7}	5
MKMI5	HPF(72)	2.1×10^{-7}	8.8×10^{-7}	4
MKN1	CVF(12)	1.5×10^{-6}	–	–
MKN2	CVF(12)	3.0×10^{-8}	–	–
MKN3	CVF(12)	5.0×10^{-8}	–	–
MKN4	CVF(12)	2.6×10^{-7}	–	–
MKN5	CVF(12)	2.9×10^{-7}	–	–
MKN6	CVF(12)	4.0×10^{-8}	–	–
MKN7	CVF(12)	1.1×10^{-8}	–	–
MKN8	CVF(12)	5.8×10^{-7}	–	–
MKN9	CVF(12)	1.2×10^{-9}	–	–
MKN10	CVF(12)	2.5×10^{-8}	9.4×10^{-8} [b]	20.3[b]

[a] H_2/CO_2 separation measurements carried out at 150 °C, under isobaric conditions using Ar as sweep gas. Feed composition H_2/CO_2/Ar:20/20/60, feed/sweep gas ratio: 1/1.
[b] H_2/C_3H_8 separation measurements were carried out instead of H_2/CO_2 after Pd nanoparticles filtration.

prolongued periods (around 48 h) and using the stabilized microemulsion as metal source. Finally, HPF (for 72 h and microemulsion as metal source), seems to be more effective as the Pd deposition appears to be uniform through the membrane even several cycles are necessary to invert the membrane position inside the steel housing. Therefore, high transmembrane pressures and the employment of microemulsions as Pd source are two imperative conditions for high quality deposition.

Once Pd microemulsion filtration is carried out, the composite membrane has to be calcined to solve the problems associated with the presence of an organic surfactant (Berol) susceptible of decomposition during permeation experiments at relative high temperatures. Figure 11 shows the TGA curve obtained with a Pd microemulsion using Protocol 1. Up to 300 °C the weight decreases almost monotonically (i.e. same slope in each heating ramp); however, above 300 °C a weight increase is observed, possibly due to the formation of PdO. The temperature for the maximum weight loss (32% weight loss) is 295 °C. The TGA curve obtained with Protocol 3 is also plotted on Figure 11. Up to 200 °C the weight loss is a 23% of the initial value, and during heating step from 200 to 250 °C, a slight weight increase of 2% is observed. This is due to the fact that Pd oxidation shifts to lower temperatures under air atmosphere. For this protocol, the temperature for the maximum weight loss is 200 °C, whereas at 350 °C, the accumulated weight loss is 27.5%.

Figure 12 shows the TGA curve corresponding to Pd microemulsion calcination using Protocol 2. Up to 150 °C the weight decreases almost linearly, remaining nearly constant until the atmosphere composition

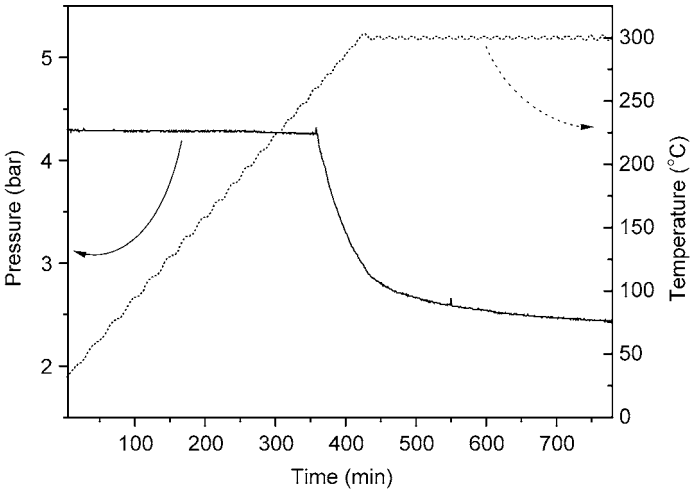

Figure 9: Transmembrane pressure evolution (at constant gas flow rate) with temperature for a A-type zeolite membrane seeded with Pd by microemulsion filtration.

shift (from 2 to 20% O_2) at 250 °C. This external perturbation is probably masking the Pd oxidation, although a slight weight increase starting at around 240 °C is observed, similar to Protocol 2. Under these conditions, the weight loss is the highest (around 50% at 300 °C); although the main contribution is in the low-temperature region, which conditions are common for all the protocols tested. As a general conclusion drawn from the TGA results, 250 °C is a suitable temperature for membrane calcination under air atmosphere to avoid PdO formation.

Table 5A and B summarize the N_2 permeances evaluated at room temperature after Pd deposition by the three different methods using 250 °C/8 h (Table 5A) or 400 °C/12 h (Table 5B) as calcination conditions. It is worth to emphasize that Method 3, denotes as HPF, proportionates better permeation results

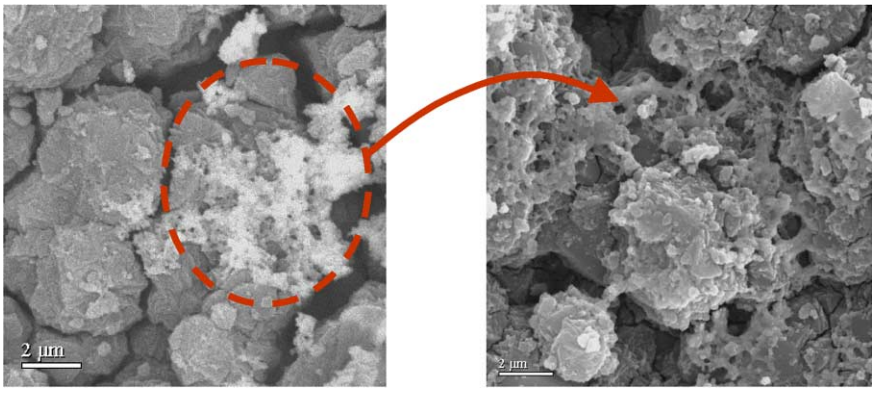

Figure 10: SEM micrographs of the external surface of a KA zeolite membrane seeded with Pd by microemulsion filtration after calcination at 400 °C: left side) general external view, right side) magnification of Pd aggregates.

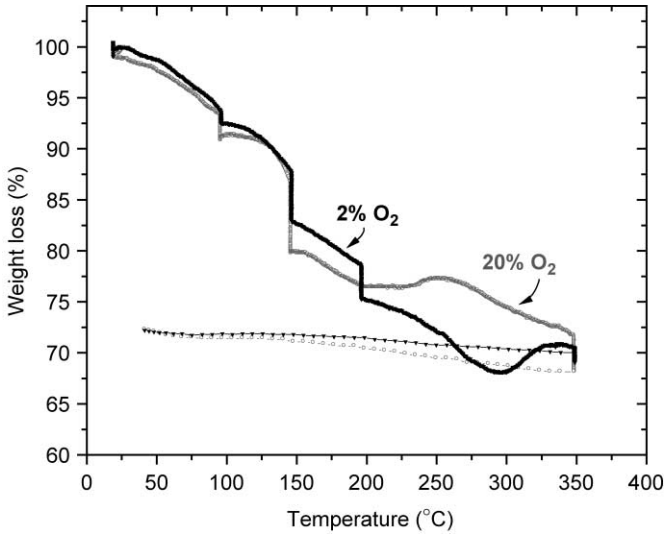

Figure 11: TGA analysis of the Pd microemulsion using conditions 1 and 3, respectively.

in terms of effective pore blockage by Pd (N_2 fluxes 6.7 times lower for HPF vs. 4.6 times for NVCF after Berol removal). Hence, HPF can be considered as the most effective deposition method among the tested. It can also be observed that when 400 °C is used as final calcination temperature, permeations increase due to the thermal cracks formation in agreement with the results already shown in Figure 9.

SEM observations (not shown here) of Pd–zeolite composite membranes calcined according to the same procedure (1 °C/min as heating rate and dwelling at 400 °C for 8 h), were also performed to investigate how the impregnation method and the elimination of the organics from the membrane surface affects the quality of the surface.

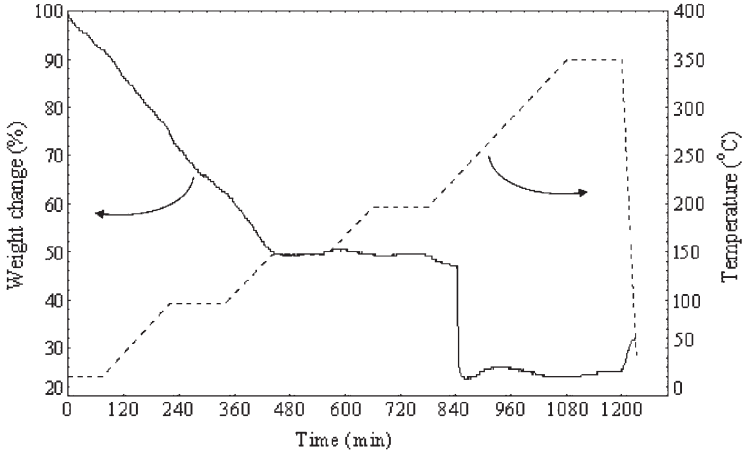

Figure 12: TGA analysis of the Pd microemulsion using condition 2.

TABLE 5A
INFLUENCE OF Pd MICROEMULSION FILTRATION METHOD OVER N_2 PERMEANCE

Sample	After zeolite synthesis (mol N_2/m^2 s Pa)	After microemulsion filtration (mol N_2/m^2 s Pa)	After berol removal[a] (mol N_2/m^2 s Pa)
MKMI2 (NCVF)	7.3×10^{-7}	1.7×10^{-8}	1.6×10^{-7}
MKMI3 (CVF)	8.7×10^{-7}	2.2×10^{-7}	1.6×10^{-7}
MNaMI1 (HPF)	6.7×10^{-8}	2.8×10^{-9}	1.0×10^{-8}

[a] Berol removal carried out at 250 °C in air for 12 h.

TABLE 5B
INFLUENCE OF Pd MICROEMULSION FILTRATION METHOD OVER N_2 PERMEANCE

Filtration method	After zeolite synthesis (mol N_2/m^2 s Pa)	After berol removal[a] (mol N_2/m^2 s Pa)
NCVF	2.0×10^{-6}	5.3×10^{-7}
CVF	2.0×10^{-6}	3.2×10^{-7}
HPF	3.4×10^{-7}	8.9×10^{-7}

[a] Berol removal carried out at 400 °C in air for 8 h.

The membrane prepared by NCVF presented a low percentage and non-uniform Pd deposition (preferential zone coverage) with Pd agglomerated particles (5–30 nm). Moreover, the high porosity on the membrane surface was mainly in forms of gaps and thick cracks due to the surfactant removal and the thermal expansion behavior. On the other hand, CVF and HPF led to a high percentage of Pd and a uniform coverage. Agglomerated Pd (5–15 nm) were observed in less extent but thermal cracks still remained.

It was really difficult to determine by SEM–EDX exactly how deep the Pd nanoparticles deposited into the zeolite layer for the just Pd seeded zeolite membranes due to the lower Pd loadings achieved. However, there were some indications that Pd nanoparticles could exist from 1 to 10 μm distance to the external surface (20 μm as zeolite membrane thickness), but mostly concentrated along the first 5 μm.

Pd deposition by impregnation + in situ reduction IRIS technique

A statistical design of IRIS experiences has been carried out to analyze systematically the influence of the operating conditions on Pd distribution over the zeolite layer. The studied variables have been the following: reaction temperature, H_2 partial pressure, reactant mode (liquid phase fed to the internal or external side) and initial state of the zeolite membrane (wetted or dried support). All the experiments have been conducted using $Pd(acac)_2$/dichloroethane solution 0.01 M, keeping both sides of the membrane at atmospheric pressure during 90 min. From the SEM–EDX analysis of the samples tested (not shown here), some qualitative conclusions are deduced. The initial wetness of the zeolite membrane decrease the deposition rate because the Pd ions have to diffuse in the liquid phase to reach the reaction interface and therefore the Pd loadings are lower but are located deeper inside. On the contrary if the membrane is initially dry, the liquid solution (water and Pd precursor) penetrates quickly by capillary forces inside the porous structure, the diffusion path is shorter and the reaction interface is closer to the external side of the membrane where the gas phase is fed. Under such conditions an external thin Pd layer with low thermal and mechanical stability tends to form. When different temperatures are compared (60 vs. 80 °C), it is observed that higher temperatures favor a deeper location of Pd (inside the macroporous support). This probably happens because at higher temperatures the dried

membrane thickness in contact with gas phase is higher and therefore the reaction interface moves to the internal side.

As a general conclusion, for a standard zeolite NaA membrane (i.e. N_2 permeation around 10^{-7} mol N_2/m^2 s Pa,), 60 °C and 50% of H_2 in the gas phase fed to the external side of the membrane appears as the most adequate operating condition for preferential deposition of Pd inside the non-selective pores of a zeolite membrane initially wetted.

Figure 13 shows the Pd and Si/Al distribution profiles as a function of the distance to the external surface for a Pd–zeolite composite membrane prepared under the above IRIS conditions. As it can be observed, Pd deposition is confined within the zeolite layer, around 10 μm thickness, for which the Si/Al atomic ratio is around 1.0. The Pd loadings vary from 98 to 25% with the external distance, indicating that Pd is preferentially deposited on the outer surface probably where the inter-crystalline pores concentration is higher.

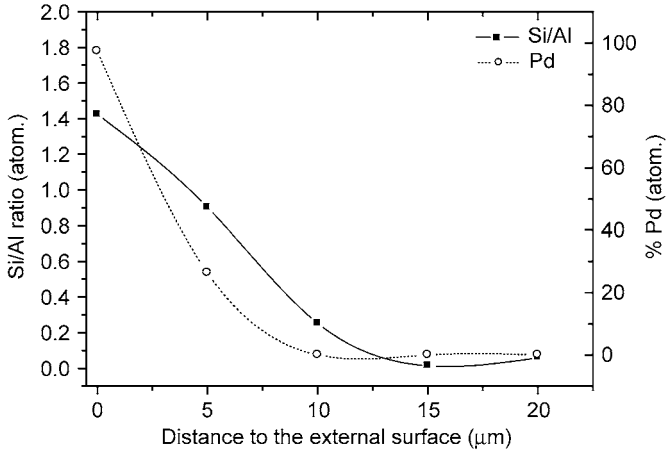

Figure 13: Pd and Si/Al radial profiles analyzed by SEM-EDX for a Pd–zeolite composite membrane prepared using "optimal" IRIS conditions.

However, successive cycles or prolongued IRIS experiences have been necessary to improve H_2 separation performance. Figure 14 shows the evolution of the consumption rate for an A-type zeolite membrane during a single IRIS experience in which the solution temperature was increased with time in order to optimize Pd blockage. The reaction temperature is a key factor which plays an important role over Pd deposition, by increasing the solvent evaporation rate and the kinetic constant for Pd reduction and decreasing the H_2 solubility in the liquid phase. Therefore, it could be expected that by increase in temperature a higher Pd deposition rate could be achieved, located preferentially on the external side of the membrane where the zeolite layer is placed. Moreover, the solution consumption rate would have to decrease along time due to progressive Pd deposition over non-zeolitic pores and the higher tortuosity of the remaining pathways. Both tendencies are corroborated in Figure 14, for which the solution consumption rate decrease from 3.6 to 0.06 cm^3/h when IRIS temperature increases from 30 to 80 °C causing a N_2 permeation reduction of 46% with respect to the value measured after NaA zeolite synthesis.

Figure 15A and B compile the H_2/CO_2 separation factor and CO_2 permeance evolution with successive cycles of impregnation + in situ reduction for different Pd–zeolite composite membranes. It is observed that the H_2/CO_2 separation factors around 3, typically obtainer after Pd seeding, increase up to 145 for

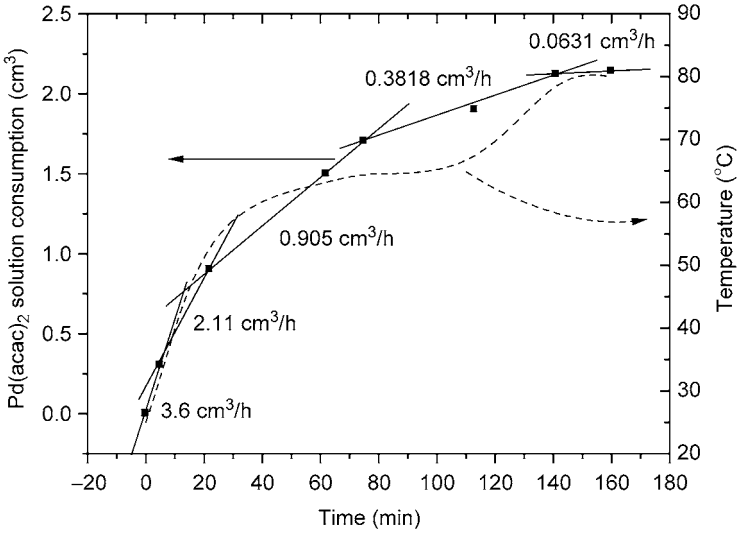

Figure 14: $Pd(acac)_2$/dichloroethane consumption rate for an IRIS experience in which the solution temperature is increased with deposition time.

the best sample (MKMI2) with successive IRIS cycles, whereas H_2 permeance decreases up to two orders of magnitude with respect to that after Pd filtration (from 1.2×10^{-6} to 9.3×10^{-9} mol H_2/Pa s m^2).

MKMI2 sample was analyzed by SEM–EDX at different radial and axial positions, and a good reproducibility was attained. Figure 16B shows the Pd, Si and Al distribution profiles for a given axial coordinate (Figure 16A). The Pd and Si/Al atomic ratio profiles follow the same tendency previously shown in Figure 13: around 8 μm of thickness, and similar zeolite layer composition and Pd loadings. According to that, the reproducibility of this Pd deposition method is rather acceptable.

CONCLUSIONS

Several issues related to the thermal treatments necessary for drying and testing of the highly hydrophilic zeolite A membranes have been solved to avoid thermal cracks due to uncontrolled loss of water. According to the detailed thermal study carried out, the maximum temperature that this type of substrates can withstand while keeping its permeance and separation properties is 350 °C. The defect size distribution estimated by permporometry analysis clearly calls to a reparation strategy by blocking the non-selective pores.

After K exchange, zeolite membranes exhibit, in general, better separation properties than their NaA counterparts, although the permeation levels usually increase due to the leaching of amorphous silica deposited onto the zeolite membrane surface. However, the contribution of non-selective pathways to gas permeation remains high and consequently, a reparation technique based on Pd deposition has been necessary for almost all membranes tested.

Pd–zeolite composite membranes have been obtained although moderate selectivities (H_2/CO_2) were achieved because the Pd clusters formed are not adequate to block the wide size distribution of defects present in the microporous zeolite layer. Further optimization is needed in all the techniques for Pd

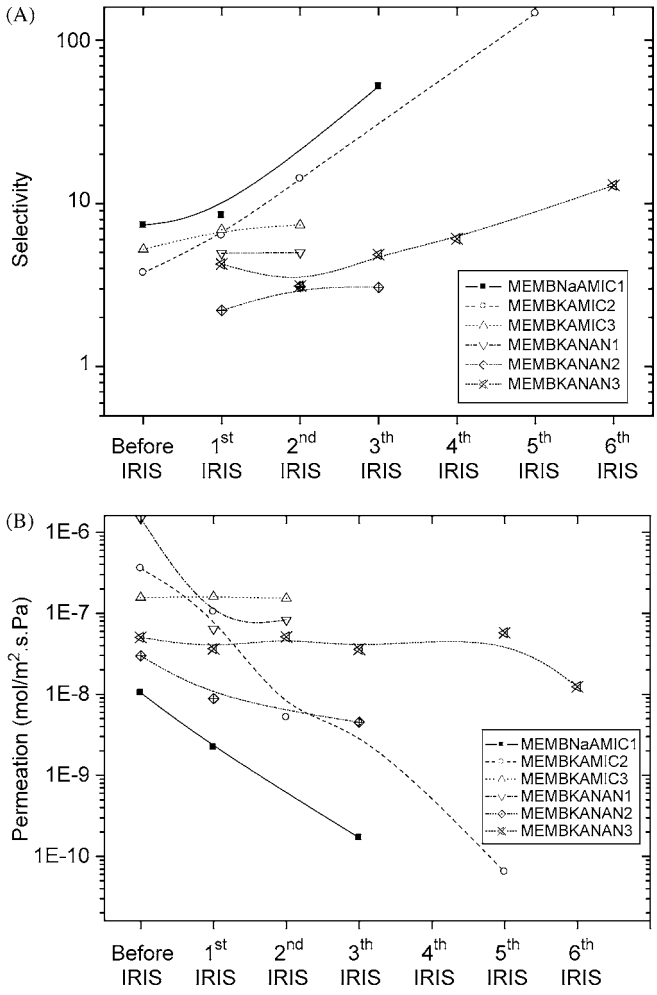

Figure 15: Evolution of H_2 separation performance with successive cycles of impregnation + in situ reduction for different Pd–zeolite composite membranes: (A) H_2/CO_2 separation factors, (B) CO_2 Permeance. Experimental conditions: 150 °C, atmospheric pressure, feed composition H_2/CO_2/Ar:20/20/60, feed/sweep gas ratio: 1/1.

deposition, particularly in the final steps necessary to complete the blockage of non-selective pathways and enhance the H_2 separation performance.

Among the different techniques used for Pd modification, the seeding with Pd microemulsion filtration followed by IRIS technique leads to the highest H_2 separation performance achieved (H_2/CO_2 selectivity values around 145). This result is probably associated with the sponge-like porous structure obtained after Berol removal at 250 °C over the Pd seeded membranes, temperature which preserves the integrity of the zeolite layer. This technique provides the best H_2-CO_2 separation reported for non-dense Pd membranes at

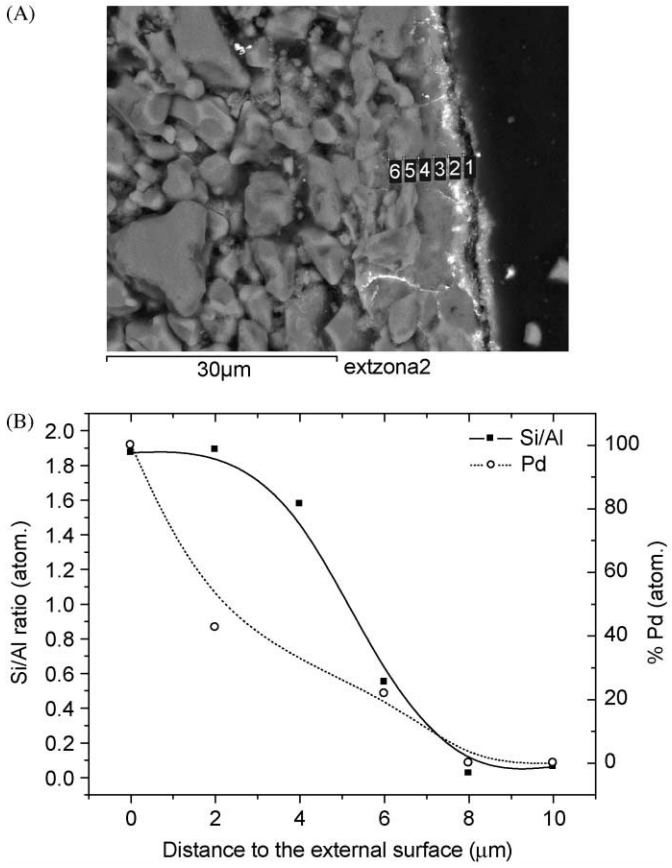

Figure 16: Pd and Si/Al radial profiles analyzed by SEM-EDX for MKMI2 sample: (A) cross section of the Pd composite zeolite membrane, (B) distribution profiles.

high temperatures, and therefore constitutes a new alternative for the development of membrane reactors usable in hydrogen fuel production.

ACKNOWLEDGEMENTS

Financial support from the EC (GRACE project) is gratefully acknowledged.

REFERENCES

1. M. Matsukata, E. Kikuchi, Zeolitic membranes: synthesis, properties, and prospects, *Bull. Chem. Soc. Jpn* **70** (1997) 2341.
2. T. Bein, Synthesis and applications of molecular sieve layers and membranes, *Chem. Mater.* **8** (1996) 1636.
3. A. Tavolaro, E. Drioli, Zeolite membranes, *Adv. Mater.* **11** (1999) 975.

4. J. Coronas, J. Santamaría, Separations using zeolite membranes, *Sep. Purif. Methods* **28** (1999) 127.
5. J. Caro, M. Noack, P. Kölsch, R. Schäfer, Zeolite membranes—state of their development and perspective, *Microporous Mesoporous Mater.* **38** (2000) 3.
6. S. Mintova, T. Bein, Nanosized zeolite films for vapor sensing applications, *Microporous Mesoporous Mater.* **50** (2–3) (2001) 159.
7. M. Vilaseca, J. Coronas, A. Cirera, A. Cornet, J.R. Morante, J. Santamaría, Use of zeolite films to improve the selectivity of reactive gas sensors, *Catal. Today* **82** (1–4) (2003) 179.
8. Y. Shan, S. Wan, J.L. Hang, A. Gavriilidis, K.L. Yeung, Design and fabrication of zeolite-based microreactors and membrane microseparators, *Microporous Mesoporous Mater.* **42** (2–3) (2001) 157.
9. X. Lin, E. Kikuchi, M. Matsukata, Preparation of Mordenite membranes on alpha-alumina tubular supports for pervaporation of water-isopropyl alcohol mixtures, *J. Membr. Sci.* **117** (1996) 163.
10. K. Kusakabe, T. Kuroda, A. Murata, S. Morooka, Formation of a Y-type zeolite membrane on a porous α-alumina, *Ind. Engng Chem. Res.* **36** (1997) 649.
11. K. Kusakabe, T. Kuroda, K. Uchino, Y. Hasegawa, S. Morooka, Gas permeation properties of ion-exchanged Faujasite-type zeolite membranes, *AIChE J.* **45** (1999) 1220.
12. T. Matsufuji, N. Nishiyama, K. Ueyae, M. Matsukata, Crystallization of Ferrierite on a porous alumina support by a vapor phase transport method, *Microporous Mesoporous Mater.* **32** (1999) 159.
13. I. Kumakiri, T. Yamaguchi, S. Nakao, Preparation of zeolite A and Faujasite membranes from a clear solution, *Ind. Engng Chem. Res.* **38** (1999) 4682.
14. L. Casado, R. Mallada, C. Téllez, J. Coronas, M. Menéndez, J. Santamaría, Preparation, characterization and pervaporation performance of mordenite membranes, *J. Membr. Sci.* **216** (1–2) (2003) 135.
15. X. Zhang, J. Wang, H. Liu, C. Liu, K. Yeung, Factors affecting the synthesis of hetero-atom zeolite Fe-ZSM-5 membrane, *Sep. Purif. Technol.* **32** (1–3) (2003) 151.
16. M.A. Rosen, D.S. Scott, Comparative efficiency assessments for a range of hydrogen production processes, *Int. J. Hydrogen Energy* **23** (1998) 653.
17. J. Shu, B.P.A. Grandjean, A. Van Neste, S. Kaliaguine, Catalytic Palladium-based membrane reactors: a review, *Can. J. Chem. Engng* **69** (1991) 1036.
18. D. Atnoor, R. Govind, Development of a composite Palladium membrane for selective hydrogen separation at high temperatures, *Ind. Engng Chem.* **30** (1991) 591.
19. S. Uemiya, T. Matsuda, E. Kikuchi, Hidrogen permeable Palladium–silver alloy membranes supported on porous ceramics, *J. Membr. Sci.* **56** (1991) 315.
20. K.L. Yeung, J.M. Sebastian, A. Varma, Novel preparation of Pd/Vycor composite membranes, *Catal. Today* **25** (1995) 231.
21. A. Li, G. Xiong, J. Gu, L. Zheng, Preparation of Pd/ceramic composite membrane 1. Improvement of the conventional preparation technique, *J. Membr. Sci.* **110** (1996) 257.
22. I.P. Mardilovich, Y. She, Y.H. Ma, M.-H. Rei, Defect free palladium membranes on porous stainless-steel support, *AIChE J.* **44** (2) (1998) 310.
23. K.L. Yeung, S.C. Christiansen, A. Varma, Palladium composite membranes by electroless plating technique relationships between plating kinetics, film microstructure and membrane performance, *J. Membr. Sci.* **159** (1999) 107.
24. Y.S. Cheng, M.A. Peña, J.L. Fierro, D.C.W. Hui, K.L. Yeung, Performance of alumina, zeolite, palladium, Pd–Ag alloy membranes for hydrogen separation from Town gas mixture, *J. Membr. Sci.* **204** (2002) 329.
25. R.S. Souleimanova, A.S. Mukasyan, A. Varma, Pd membranes formed by electroless plating with osmosis: H_2 permeation studies, *AIChE J.* **48** (2) (2002) 262.
26. I.P. Mardilovich, E. Engwall, Y.H. Ma, Dependence of hydrogen flux on the pore size and plating surface topology of asymmetric Pd-porous stainless steel membranes, *Desalination* **144** (1–3) (2002) 85.
27. E. Piera, J. Coronas, M. Menéndez, J. Santamaría, High separation selectivity with imperfect zeolite membranes, *Chem. Commun.* **14** (1999) 1309.
28. M. Nomura, T. Yamaguchi, S. Nakao, Silicalite membranes modified by counter diffusion CVD technique, *Ind. Engng Chem. Res.* **36** (1997) 4217.
29. Y. Yan, M.E. Davis, G.R. Gavalas, Preparation of highly selective zeolite ZSM-5 membranes by a post-synthetic coKing treatment, *J. Membr. Sci.* **123** (1997) 95.

30. G. Xomeritakis, A. Gouzinis, S. Nair, T. Okubo, M. He, R.M. Overney, M. Tsapatsis, Growth, microstructure, and permeation properties of supported zeolite (MFI) films and membranes prepared by secondary growth, *Chem. Engng Sci.* **54** (15–16) (1999) 3521.
31. S. Nair, Z. Lai, V. NikolaKis, G. Xomeritakis, G. Bonilla, M. Tsapatsis, Separation of close-boiling hydrocarbon mixtures by MFI and FAU membranes made by secondary growth, *Microporous Mesoporous Mater.* **48** (1–3) (2001) 219.
32. G. Li, E. Kikuchi, M. Matsukata, The control of phase and orientation in zeolite membranes by the secondary growth method, *Microporous Mesoporous Mater.* **62** (3) (2003) 211.
33. S. Yamazaki, K. Tsutsumi, Synthesis of A-type zeolite membrane using a plate heater and its formation mechanism, *Microporous Mesoporous Mater.* **37** (2000) 67.
34. I. Kumakiri, Preparation and permeation mechanism of zeolite membranes. *PhD Dissertation*, The University of Tokio (Japan) (2000).
35. H. Richter, I. Voight, P. Fischer, P. Puhlfürß, Preparation of zeolite membranes on the inner surface of ceramic tubes and capillaries, *Sep. Purif. Technol.* **32** (2003) 133.
36. A. Erdem-Senatalar, M. Tatlier, M. Ürgen, Preparation of zeolite coatings by direct heating of the substrates, *Microporous Mesoporous Mater.* **32** (1999) 331.
37. T. Cetin, M. Tatlier, A. Erdem-Senatalar, U. Demirler, M. Ürgen, Lower temperatures for the preparation of thinner zeolite A coatings, *Microporous Mesoporous Mater.* **47** (2001) 1.
38. F. Tiscareño-Lechuga, C. Téllez, M. Menéndez, J. Santamaría, A novel device for preparing zeolite—A membranes under a centrifugal force field, *J. Membr. Sci.* **212** (1–2) (2003) 135.
39. K. Aoki, K. Kusakabe, S. Morooka, Separation of gases with an A-type zeolite membrane, *Ind. Engng Chem. Res.* **39** (2000) 2245.
40. X. Xu, W. Yang, J. Liu, X. Chen, L. Lin, N. Stroh, H. Brunner, Synthesis and gas permeation properties of an NaA zeolite membrane, *Chem. Commun.* (2000) 603.
41. X. Xu, W. Yang, J. Liu, L. Lin, Synthesis of a high-permeance NaA zeolite membrane by microwave heating, *Adv. Mater.* **12** (2000) 195.
42. K. Okamoto, H. Kita, K. Horii, K. Tanaka, M. Kondo, Zeolite NaA membrane: preparation, single gas permeation, and pervaporation and vapor permeation of water/organic liquid mixture, *Ind. Engng Chem. Res.* **40** (2001) 163.
43. X. Xu, W. Yang, J. Liu, L. Lin, Synthesis of NaA zeolite membrane by microwave heating, *Sep. Purif. Technol.* **25** (2001) 241.
44. Y.H. Ma, Y. Zhou, R. Poladi, E. Engwall, The synthesis and characterization of zeolite A membranes, *Sep. Purif. Technol.* **25** (2001) 235.
45. X. Xu, W. Yang, J. Liu, L. Lin, Synthesis and perfection evaluation of NaA zeolite membrane, *Sep. Purif. Technol.* **25** (2001) 475.
46. H. Kita, K. Korii, Y. Ohtoshi, K. Tanaka, K. Okamoto, Synthesis of a zeolite NaA membrane for pervaporation of water/organic liquid mixtures, *J. Mater. Sci. Lett.* **14** (1995) 206.
47. J.J. Jafar, P.M. Budd, Separation of alcohol/water mixtures by pervaporation through zeolite A membranes, *Microporous Mater.* **12** (1997) 305.
48. M. Kondo, M. Komori, H. Kita, K. Okamoto, Tubular-type pervaporation module with zeolite NaA membrane, *J. Membr. Sci.* **133** (1997) 133.
49. D. Shah, K. Kissick, A. Ghorpade, R. Hannah, D. Bhattacharyya, Pervaporation of alcohol–water and dimethylformamide–water mixtures using hydrophilic zeolite NaA membranes: mechanisms and experimental results, *J. Membr. Sci.* **179** (2000) 185.
50. Y. Morigami, M. Kondo, J. Abe, H. Kita, K. Okamoto, The first large-scale pervaporation plant using tubular-type module with zeolite NaA membrane, *Sep. Purif. Technol.* **25** (2001) 251.
51. A.W.C. van den Berg, L. Gora, J.C. Jansen, M. Makkee, Th. Maschmeyer, Zeolite A membranes synthesized on a UV-irradiated TiO_2 coated metal support: the high pervaporation performance, *J. Membr. Sci.* **224** (1–2) (2003) 29.
52. F. Morón, M.P. Pina, E. Urriolabeitia, M. Menéndez, J. Santamaría, Preparation and characterization of Pd–zeolite composite membranes for hydrogen separation, *Desalination* **147** (2002) 425.
53. D.W. Breck, Zeolite Molecular Sieves, Robert E. Krieger Publishing Company, Malabar, Florida (USA), 1984.
54. M. Boutonnet, J. Kizling, P. Stenius, G. Maire, The preparation of monodispersed colloidal metal particles from microemulsions, *Colloid. Surface* **5** (1982) 209.

55. R. Touroude, P. Bernhardt, G. Maire, J. Kizling, M. Boutonnet-Kizling, P. Stenius, Solubilization and reduction of Pt and Pd salts in nonionic microemulsions: characterisation by light scattering and EXAFS, in: Stig E. Friberg, B. Lindman (Eds.), *Organized Solutions, Surfactants in Science and Technology*, Marcel Dekker, New York, 1992, p. 357.
56. J. Kizling, M. Boutonnet-Kizling, P. Stenius, R. Touroude, G. Maire, Preparation of colloidal metals by reduction or precipitation in microheterogenous fluids, in: R.A. Mackay, J. Texter (Eds.), *Electrochemistry in Colloids and Dispersions*, VCH Publishers, New York, 1992, pp. 333–344.
57. M.T. Reetz, M. Maase, Redox-Controlled size-selective fabrication of nanostructures transition metal colloids, *Adv. Mater.* **11** (1999) 773.
58. C. Dueso, M.P. Pina, E.P. Urriolabeitia, R. Navarro, A. Larrea, M. Menéndez, J. Santamaría, Preparation of Pd nanoparticles for the synthesis of new materials, *Book of Abstracts of the 9th Mediterranean Congress of Chemical Engineering*, Barcelona, España, 2002, 258.
59. H. Raeder, R. Bredesen, G. Creham, S. Miachon, J.A. Dalmon, A. Pintar, J. Levec, E.G. Torp, A wet air oxidation process using a catalytic membrane contactor, *Sep. Purif. Technol.* **32** (2003) 349.
60. S. Miachon, V. Pérez, G. Creham, E.G. Torp, H. Raeder, R. Bredesen, J.A. Dalmon, Comparison of a contactor catalytic membrane reactor with a conventional reactor: example of wet air oxidation, *Catal. Today* **82** (1–4) (2003) 75.
61. K. Keizer, R.J.R. Ulhorn, R.J. Van Vuren, A.J. Burgraaf, Gas separations properties in microporous modifies Al_2O_3 membranes, *J. Membr. Sci.* **39** (1988) 285.
62. http://www.iza-structure.org.